

SOFT LITHOGRAPHY

Younan Xia and George M. Whitesides

Department of Chemistry and Chemical Biology, Harvard University, Cambridge, Massachusetts 02138; e-mail: gwhitesides@gmwgroup.harvard.edu

KEY WORDS: patterning, microfabrication, nanofabrication, elastomers, self-assembled monolayers

ABSTRACT

Soft lithography represents a non-photolithographic strategy based on self-assembly and replica molding for carrying out micro- and nanofabrication. It provides a convenient, effective, and low-cost method for the formation and manufacturing of micro- and nanostructures. In soft lithography, an elastomeric stamp with patterned relief structures on its surface is used to generate patterns and structures with feature sizes ranging from 30 nm to 100 μm . Five techniques have been demonstrated: microcontact printing (μCP), replica molding (REM), microtransfer molding (μTM), micromolding in capillaries (MIMIC), and solvent-assisted micromolding (SAMIM). In this chapter we discuss the procedures for these techniques and their applications in micro- and nanofabrication, surface chemistry, materials science, optics, MEMS, and microelectronics.

INTRODUCTION

Microfabrication, through its role in microelectronics and optoelectronics, is an indispensable contributor to information technology (1). It is also ubiquitous in the fabrication of sensors (2), microreactors (3), combinatorial arrays (4), microelectromechanical systems (MEMS) (5), microanalytical systems (6, 7), and micro-optical systems (8, 9). Microfabrication uses a variety of patterning techniques (10, 11); the most powerful of these is photolithography, and essentially all integrated circuits are fabricated using this technology (10-12).

Projection photolithography is a parallel process (12): The entire pattern of the photomask can be projected onto a thin film of photoresist at the same time. State-of-the-art photolithographic techniques are capable of mass-producing patterned structures in thin films of photoresists with feature sizes as small as

~250 nm (13, 14), and it is plausible that the same technology can be extended to features as small as ~100 nm in the future by use of a combination of deep UV light (e.g. 193 nm ArF excimer laser or 157 nm F₂ excimer laser) and improved photoresists (13). As far as we now foresee, however, these optical methods cannot surmount the so-called 100 nm barrier—a critical value in the reduction of feature sizes set by a combination of optical diffraction and short-wavelength cutoff to the transparency of the optical materials used as lenses. Advanced lithographic techniques currently being explored as potential substitutes for conventional photolithography in the regime <100 nm include extreme UV (EUV) lithography, soft X-ray lithography, e-beam writing, focused ion beam (FIB) writing, and proximal-probe lithography (15, 16). These techniques have the capability to generate extremely small features (as small as a few nm), but their development into economical methods for mass-production (or manufacturing) of nanostructures still requires substantial effort: EUV and X-ray techniques, for example, require the development of reflective optics and/or new types of masks, and arrays of beams or some form of flood illumination rather than a single beam must be developed in e-beam or FIB writing; all require new ideas for mask maintenance and repair and for dealing with problems such as nonplanarity in the substrate.

Although photolithography is the dominant technology, even for large (μm -scale) features, it is not always the best and/or the only option for all applications: For example, it is not an inexpensive technology (11–14); it is poorly suited for patterning nonplanar surfaces; it provides almost no control over the chemistry of the surface and hence is not very flexible in generating patterns of specific chemical functionalities on surfaces (e.g. for anchorage-dependent tissue culture or combinatorial chemistry); it can generate only two-dimensional microstructures; and it is directly applicable only to a limited set of photosensitive materials (e.g. photoresists) (17). The characteristics of photolithography are such that it is relatively little used for microfabrication based on materials other than photoresists; to work with other materials it is necessary to attach chromophores or add photosensitizers, and neither type of procedure is convenient.

We have developed an alternative, non-photolithographic set of microfabrication methods that we call soft lithography (18–20) because all its members share the common feature of using a patterned elastomer as the stamp, mold, or mask (rather than a rigid photomask) to generate micropatterns and microstructures. We have explored six such techniques: microcontact printing (μCP) (21), replica molding (REM) (22), microtransfer molding (μTM) (23), micro-molding in capillaries (MIMIC) (24), solvent-assisted micromolding (SAMIM) (25), and phase-shift photolithography (26). Cast molding (27, 28), embossing (29, 30), and injection molding (31–33) are also part of this area of technology and have been developed by others.

Table 1 Comparison between photolithography and soft lithography

	Photolithography	Soft lithography
Definition of patterns	Rigid photomask (patterned Cr supported on a quartz plate)	Elastomeric stamp or mold (a PDMS block patterned with relief features)
Materials that can be patterned directly	Photoresists (polymers with photo- sensitive additives) SAMs on Au and SiO ₂	Photoresists ^{a,e} SAMs on Au, Ag, Cu, GaAs, Al, Pd, and SiO ₂ ^a Unsensitized polymers ^{b-e} (epoxy, PU, PMMA, ABS, CA, PS, PE, PVC) Precursor polymers ^{c,d} (to carbons and ceramics) Polymer beads ^d Conducting polymers ^d Colloidal materials ^{a,d} Sol-gel materials ^{c,d} Organic and inorganic salts ^d Biological macromolecules ^d
Surfaces and structures that can be patterned	Planar surfaces 2-D structures	Both planar and nonplanar Both 2-D and 3-D structures
Current limits to resolution	~250 nm (projection) ~100 nm (laboratory)	~30 nm ^{a,b} , ~60 nm ^e , ~1 μm ^{d,e}
Minimum feature size	~100 nm (?)	10 (?) - 100 nm

^{a-e}Made by (a) μCP, (b) REM, (c) μTM, (d) MIMIC, (e) SAMIM. PU:polyurethane; PMMA: poly(methyl methacrylate); ABS: poly(acrylonitrile-butadiene-styrene); CA: cellulose acetate; PS: polystyrene; PE: polyethylene; and PVC: poly(vinyl chloride)

Table 1 compares the advantages and disadvantages of conventional photolithography and soft lithography. Soft lithographic techniques are low in capital cost, easy to learn, straightforward to apply, and accessible to a wide range of users. They can circumvent the diffraction limitations of projection photolithography; they provide access to quasi-three-dimensional structures and generate patterns and structures on nonplanar surfaces; and they can be used with a wide variety of materials and surface chemistries. The aim of this review is to describe the principles, processes, materials, applications, and limitations of soft lithographic techniques. We discuss how these non-photolithographic techniques have been used to produce patterns and structures with lateral dimensions from ~30 nm to ~500 μm. We especially want to illustrate the diversity of molecules and materials that can be patterned by these techniques. We also present issues and problems in soft lithographic techniques that

remain to be solved, for example, deformation of the elastomeric stamp or mold, density of defects in the formed pattern, and difficulty in high-resolution registration.

THE KEY ELEMENT OF SOFT LITHOGRAPHY

An elastomeric block with patterned relief structures on its surface is the key to soft lithography. We have been using poly(dimethylsiloxane) (PDMS) elastomers (or silicone rubbers) in most demonstrations; we and other groups have also used elastomers such as polyurethanes, polyimides, and cross-linked Novolac™ resins (a phenol formaldehyde polymer) (21). Poly(dimethylsiloxanes) have a unique combination of properties resulting from the presence of an inorganic siloxane backbone and organic methyl groups attached to silicon (34). They have very low glass transition temperatures and hence are fluids at room temperature. These liquid materials can be readily converted into solid elastomers by cross-linking. The formulation, fabrication, and applications of PDMS elastomers have been extensively studied and are well-documented in the literature (34). Prepolymers and curing agents are commercially available in large quantities from several companies: for example, Dow Corning and Hüls America.

The elastomeric stamp or mold is prepared by cast molding (27): A prepolymer of the elastomer is poured over a master having relief structure on its surface, then cured and peeled off. The master is, in turn, fabricated using microlithographic techniques such as photolithography, micromachining, e-beam writing, or from available relief structures such as diffraction gratings (35), TEM grids (21), polymer beads assembled on solid supports (35), and relief structures etched in metals or Si (35, 36). Figure 1 illustrates the procedure for fabricating PDMS stamps. The master is silanized by exposure to the vapor of $\text{CF}_3(\text{CF}_2)_6(\text{CH}_2)_2\text{SiCl}_3$ for ~ 30 min; each master can be used to fabricate more than 50 PDMS stamps. The PDMS elastomer that we usually use is Sylgard™ 184 obtained from Dow Corning. It is supplied as a two-part kit: a liquid silicon rubber base (i.e. a vinyl-terminated PDMS) and a catalyst or curing agent (i.e. a mixture of a platinum complex and copolymers of methylhydrosiloxane and dimethylsiloxane). Once mixed, poured over the master, and heated to elevated temperatures, the liquid mixture becomes a solid, cross-linked elastomer in a few hours via the hydrosilylation reaction between vinyl ($\text{SiCH}=\text{CH}_2$) groups and hydrosilane (SiH) groups (34).

We use elastomers because they can make conformal contact with surfaces (even those that are nonplanar on the sub- μm scale) over relatively large areas, and because they can be released easily from rigid masters or from complex, quasi-three-dimensional structures that are being molded. In addition to its

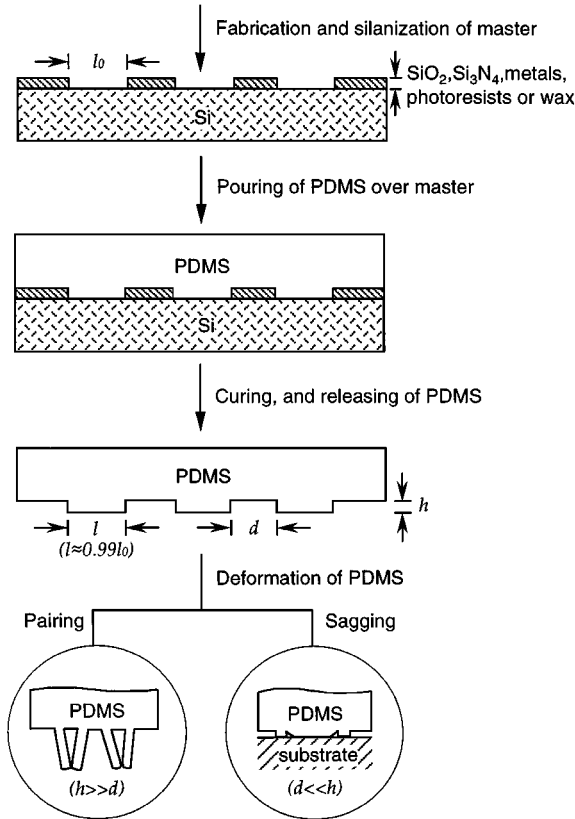


Figure 1 Schematic illustration of the procedure for fabricating PDMS stamps from a master having relief structures on its surface.

elasticity, the PDMS elastomer also has other properties (34) that makes it extremely useful in soft lithography: (a) The PDMS provides a surface that has a low interfacial free energy (~ 21.6 dyn/cm) and good chemical stability; most molecules or polymers being patterned or molded do not adhere irreversibly to, or react with, the surface of PDMS. (b) The PDMS is not hydroscopic; it does not swell with humidity. (c) The PDMS membrane passes gas easily. (d) The PDMS elastomer has good thermal stability (up to $\sim 186^\circ\text{C}$ in air); prepolymers being molded can be cured thermally. (e) The PDMS elastomer is optically transparent down to ~ 300 nm; prepolymers being molded can also be cured by UV cross-linking. (f) The PDMS elastomer is isotropic and homogeneous; stamps or molds made from this material can be deformed mechanically

to manipulate the patterns and relief structures in their surfaces (22, 37, 38). The Sylgard™ 184 elastomer has itself been used to construct elastomeric optical elements for adaptive optics (39–42) and for photomasks for phase-shift (26, 43) and conventional photolithography (44). (g) The elastomeric PDMS is durable when used as a stamp; we can use a PDMS stamp many (>50) times over a period of several months without noticeable degradation in performance. (h) The interfacial properties of PDMS elastomer can be changed readily either by modifying the prepolymers or by treating the surface with plasma, followed by the formation of siloxane SAMs (45, 46), to give appropriate interfacial interactions with materials that themselves have a wide range of interfacial free energies.

PDMS also presents a number of technical problems (Figure 1) for soft lithography; these problems remain to be solved before soft lithography becomes a general strategy for microfabrication. First, PDMS shrinks by $\sim 1\%$ upon curing; and the cured PDMS can be readily swelled by a number of nonpolar organic solvents such as toluene and hexane (34). Second, the elasticity and thermal expansion of PDMS make it difficult to get high accuracy in registration across a large area and may limit the utility of soft lithography in multilayer fabrication and/or nanofabrication. Third, the softness of an elastomer limits the aspect ratio of microstructures in PDMS. For example, the representative ranges of values for the dimensions (h , d , and l in Figure 1) are 0.2–20, 0.5–200, and 0.5–200 μm , respectively. When the aspect ratio (h/l) is too high or too low, the elastomeric character of PDMS will cause the microstructures in PDMS to deform or distort and generate defects in the pattern (Figure 1). Delamarche et al have shown that the aspect ratio of the relief features in PDMS must be between 0.2 and 2 in order to obtain defect-free stamps or molds (47). The sagging of PDMS caused by compressive forces between the stamp and the substrate excludes the use of μCP for patterns with widely separated ($d \geq 20h$) features, unless nonfunctional posts can be introduced into the design to support the noncontact regions or unless the stamp can be backed with a rigid support.

We and several other groups are seeking solutions to these technical problems. For example, Delamarche et al found that the paired lines (Figure 1) in PDMS could be restored by washing the surface with an $\sim 1\%$ aqueous solution of sodium dodecylsulfate (SDS), followed by a rinse with heptane (47). Rogers et al recently showed that the Moiré technique could be used to monitor distortions of PDMS stamps or molds during soft lithography and that the maximum distortions could be reduced to less than 1 μm over areas of $\sim 1 \text{ cm}^2$ by using thin PDMS stamps supported on rigid substrates such as glass plates (48).

We have used PDMS blocks having relief patterns on their surfaces in a number of different processes for patterning: for example, as stamps to print patterns of self-assembled monolayers (SAMs) on appropriate substrates (21);

as molds to form microstructures (both supported and free-standing) of various materials (22–25); and as photomasks to transfer patterns into thin films of photoresist using contact phase-shift photolithography (26, 43) or conventional UV photolithography (44).

MICROCONTACT PRINTING (μ CP)

The concept underlying μ CP is straightforward: It uses the relief pattern on the surface of a PDMS stamp to form patterns of self-assembled monolayers (SAMs) on the surfaces of substrates by contact. Microcontact printing differs from other printing methods (49) in the use of self-assembly (especially, the use of SAMs) to form micropatterns and microstructures of various materials.

Self-Assembly and Self-Assembled Structures

The concept of self-assembly (50, 51) has been largely stimulated by the study of biological processes: for example, folding of proteins and t-RNAs (52), formation of the DNA double-helix (53), and formation of the cell membranes from phospholipids (54). Self-assembly is the spontaneous aggregation and organization of subunits (molecules or meso-scale objects) into a stable, well-defined structure via noncovalent interactions. The information that guides the assembly is coded in the properties (e.g. topologies, shapes, and surface functionalities) of the subunits; the individual subunits will reach the final structure simply by equilibrating to the lowest energy form. Because the final self-assembled structures are close to or at thermodynamic equilibrium, they tend to form spontaneously and to reject defects. Thus self-assembly provides a simple route to certain types of structures. The obvious technical challenges to extending current photolithography to the fabrication of nanostructures and three-dimensional microstructures are such that it is now possible to at least consider self-assembly as an approach to micro- and nanofabrication. We and other groups have developed a variety of strategies of self-assembly and have employed them to fabricate two- and three-dimensional structures with dimensions ranging from molecular (55, 56), through mesoscopic (57), to macroscopic sizes (58, 59).

Self-Assembled Monolayers (SAMs)

Self-assembled monolayers are one of the most intensively studied examples of nonbiological self-assembling systems (60). SAMs can be easily prepared by immersion of a substrate in the solution containing a ligand $Y(\text{CH}_2)_n\text{X}$ reactive toward the surface, or by exposure of the substrate to the vapor of a reactive species. The thickness of a SAM can be controlled by change in the number (n) of methylene groups in the alkyl chain. The surface properties of

the monolayer can be easily modified by changing the head group, X (61). The selectivity in the binding of the anchoring group, Y, toward different substrates is a major limitation of this method for forming thin films: Some surfaces (e.g. Au and Ag) are much easier to form SAMs on than are other (metal oxides). This selectivity is, nevertheless, useful for orthogonal assembly—formation of different SAMs on different materials from a single solution containing different ligands or containing a ligand with two different terminal groups (62).

SAMs exhibit many attractive characteristics: ease of preparation, good stability under ambient laboratory conditions, relatively low densities of defects in the final structures, and amenability to application in controlling interfacial (physical, chemical, electrochemical, and biochemical) properties. They have been extensively reviewed in the literature (63–66). The best-established systems of SAMs are those of alkanethiolates on Au (67) and Ag (68), and alkylsiloxanes on hydroxyl-terminated surfaces such as Si/SiO₂, Al/Al₂O₃, glass, mica, and plasma-treated polymers (60, 69, 70). Less-well-characterized systems of SAMs include alkyl groups directly bound to Si (71, 72); alkanethiolates on Cu (73), GaAs (74), and InP (75); alkanesulfonates (76) and alkylphosphines (77) on Au; alkanethiolates on Pd (78); alkylisonitriles on Pt (79); carboxylic (80) and hydroxamic (81) acids on metal oxides; alkylphosphates on ZrO₂ (82); and alkylphosphonic acids on In₂O₃/SnO₂ (ITO) (62).

Alkanethiolates (CH₃(CH₂)_nS⁻) on Au is the best characterized and understood system of SAMs (67). The process by which they are formed on reaction of alkanethiols (in solution or vapor phase) and gold is assumed to occur with loss of dihydrogen. The sulfur atoms of alkanethiolates form a commensurate overlayer on Au(111) with a ($\sqrt{3} \times \sqrt{3}$)R30° structure. The alkyl chains extend from the plane of the surface in a nearly all-*trans* configuration. They are, on average, tilted approximately 30° from the normal to the surface to maximize the van der Waals interactions between adjacent methylene groups (see the inset of Figure 2). Surfaces represented by SAMs of alkanethiolates on Au are widely used as model systems to study interfacial phenomena such as wetting (61), adhesion (83), nucleation (84), protein adsorption (85–87), and cell attachment (86, 87). They have also been used as active elements to fabricate sensors and biosensors (88, 89).

Microcontact Printing of SAMs

Many applications of SAMs in surface chemistry and microfabrication require SAMs patterned in the plane of the surface with feature sizes at least on the μm scale. A variety of techniques have been explored for accomplishing this goal that include microcontact printing (μCP) with elastomeric stamps (21, 84, 90–93); photochemical oxidation (94–96), activation (97–99), or cross-linking (100) with UV light; and writing with an e-beam (101–103), focused ion beam (FIB) (104), neutral metastable atom beam (105–107), or sharp stylus

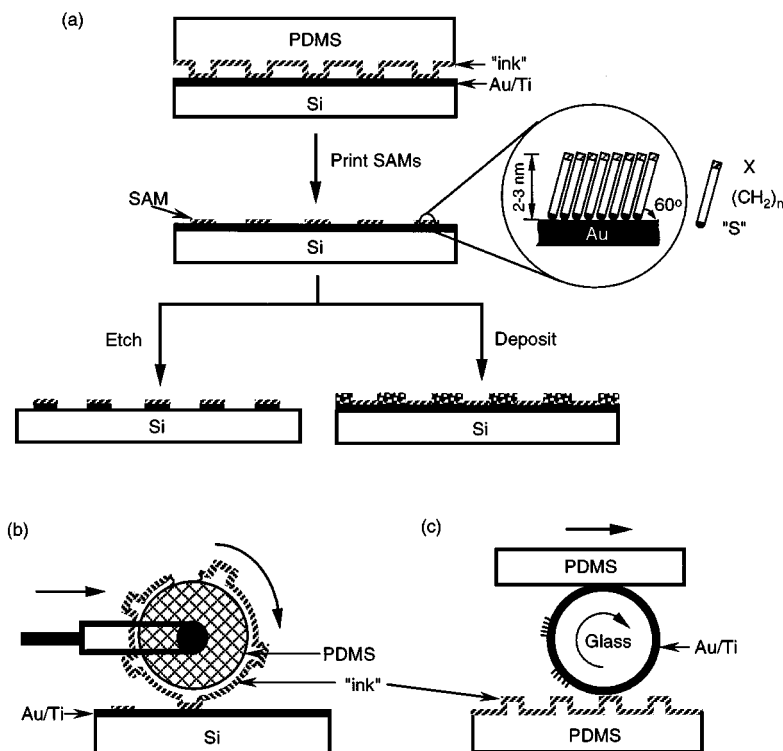


Figure 2 Schematic procedures for μ CP of hexadecanethiol (HDT) on the surface of gold: (a) printing on a planar surface with a planar stamp (21), (b) printing on a planar surface over large areas with a rolling stamp (128), and (c) printing on a nonplanar surface with a planar stamp (174).

(108, 109). This review focuses on microcontact printing because it seems to offer the most interesting combination of convenience and new capabilities.

We have developed three different configurations (Figure 2) for carrying out μ CP on substrates with different geometric parameters (91–93). The general principles and procedures are the same. In μ CP of alkanethiols on Au, for example, the PDMS stamp is wetted with an “ink” (typically, an ~ 2 -mM solution of hexadecanethiol in ethanol) and is brought into contact with the surface of Au for 10–20 s. The hexadecanethiol ($\text{CH}_3(\text{CH}_2)_{15}\text{SH}$) transfers from the stamp to the gold upon contact, forms a hexadecanethiolate ($\text{CH}_3(\text{CH}_2)_{15}\text{S}^-$), and generates patterns of SAMs on the surface of gold.

The success of μ CP rests on two characteristics of the system: the rapid formation of a highly ordered SAM and the autophobicity of the SAM that can block the spreading of the ink across the surface (110). The formation of SAMs

of alkanethiolates on gold is relatively fast. For example, highly ordered SAMs of hexadecanethiolate can form on gold within minutes after the gold substrate is immersed in an ~ 2 -mM solution of hexadecanethiol in ethanol (63). The formation of highly ordered SAMs of alkanethiolates during μ CP may occur in seconds. Biebuyck et al recently showed that a contact time > 0.3 s (~ 100 -mM solution of dodecanethiol in ethanol) was enough to form highly ordered SAMs on Au(111) that were indistinguishable from those formed by equilibration in solution. For μ CP with an ~ 2 -mM solution of hexadecanethiol in ethanol, a contact time of 10–20 s is usually used (92, 111). We found that longer contact time (> 30 s) usually resulted in the destruction of the pattern due to the transport of hexadecanethiol from the stamp to the surface in noncontact regions through the vapor phase (112).

Kumar et al first demonstrated the concept of μ CP; they used the system of SAMs of alkanethiolates on Au (21, 84). We and other groups later extended this technique to a number of other systems including SAMs of alkanethiolates on Ag (113–115), SAMs of alkanethiolates on Cu (116, 117), SAMs of alkylsiloxanes on HO-terminated surfaces (118–121), SAMs of alkanethiolates on Pd (L Goetting, unpublished data), and SAMs of RPO_3H_2 on Al (L Goetting, unpublished data). Microcontact printing has also been used to form patterns of colloidal Pd particles on Si/SiO₂ and polymers (122, 123), and patterns of protonic acids on thin (1–10 μm thick) films of chemically amplified photoresists (Y Xia, unpublished data) or sol-gel materials (124). Microcontact printing of hexadecanethiol on evaporated thin (10–200 nm thick) films of Au or Ag appears to be the most reproducible process. Both systems give highly-ordered SAMs, with a low density of defects. Unfortunately, gold and silver are not compatible with microelectronic devices based on Si (125), although they can be used as electrodes or conductive wires in many applications. Currently, μ CP of SAMs of siloxanes on Si/SiO₂ is substantially less tractable than μ CP of SAMs of alkanethiolates on Au or Ag: It usually gives disordered SAMs, and in some cases, submonolayers and multilayers (121). One of the future directions of this area will be the development of systems in which highly ordered SAMs can be formed directly on the surfaces of inorganic semiconductors easily, rapidly, and reproducibly.

Patterned SAMs as Resists in Selective Wet Etching

SAMs that are 2–3 nm thick do not have the durability to serve as resists for pattern transfer in conventional reactive ion etching (RIE). However, some have the ability to protect the underlying substrates effectively from attack by certain wet etchants (84, 126). We have shown that aqueous solutions containing $\text{K}_2\text{S}_2\text{O}_3/\text{K}_3\text{Fe}(\text{CN})_6/\text{K}_4\text{Fe}(\text{CN})_6$ or aqueous cyanide solution saturated with O_2 are effective for use with patterned SAMs of alkanethiolates on Au

and Ag (84, 126); that aqueous solutions containing FeCl_3 and HCl (or NH_4Cl) are effective for use with patterned SAMs of alkanethiolates on Cu (116); and that aqueous solutions containing HCl/ HNO_3 are effective for patterned SAMs of alkanethiolates on GaAs (E Kim, unpublished data) or Pd (L Goetting, unpublished data). Previous studies have demonstrated many other wet etchants for these and other materials, and these etchants remain to be examined in conjunction with SAMs (127).

Figure 3*a–f* shows SEM images of several test patterns of Ag (113, 128), Au (126), and Cu (118) that were generated using μCP with hexadecanethiol, followed by selective wet etching. These test patterns represent the level of complexity, perfection, and scale that can be produced routinely by this procedure. Microcontact printing, like photolithography, is an inherently parallel process. It can pattern the entire surface of the substrate in contact with the stamp at the same time. It may be useful in large-area patterning. In their initial demonstration, Xia et al patterned 3-inch wafers ($>50\text{ cm}^2$ in area) with submicron features (Figure 2*b*) in a single impression by using a cylindrical rolling PDMS stamp (128).

The minimum feature size that can be generated by μCP is mainly determined by the material properties of the stamp rather than by optical diffraction and/or the opacity of optical materials (129). Thus microcontact printing has the capability to produce features with lateral dimensions $<100\text{ nm}$. The smallest features fabricated to date with a combination of μCP of SAMs and wet etching are trenches etched in Au that are $\sim 35\text{ nm}$ wide separated by $\sim 350\text{ nm}$ (93). The minimum feature size that can be achieved by μCP remains to be defined, and a systematic study on the interactions between the stamp and the substrate will be useful for the optimization of the properties of the elastomer for use in the $<100\text{ nm}$ regime.

The patterned structures of metals formed using a combination of μCP and selective etching can be used directly as arrays of microelectrodes or as diffractive optical components (84). They can also be used as secondary masks in the etching of the underlying substrates such as SiO_2 , Si, and GaAs using wet etches or RIE (130–132). Figure 3 (*g, h*) shows SEM images of microstructures that were generated in Si using anisotropic etching of Si(100) with patterns of Ag (44) or Au (133) as the masks. Although microstructures of Si fabricated this way cannot be used for fabricating microelectronic devices, they should be directly applicable to the fabrication of microreactors, microanalytical systems, MEMS, solar cells, and diffractive optical components.

Patterned SAMs as Templates in Selective Deposition

The initial products of μCP are patterned SAMs, but the materials that can be patterned using μCP are not limited to SAMs. By modifying the interfacial

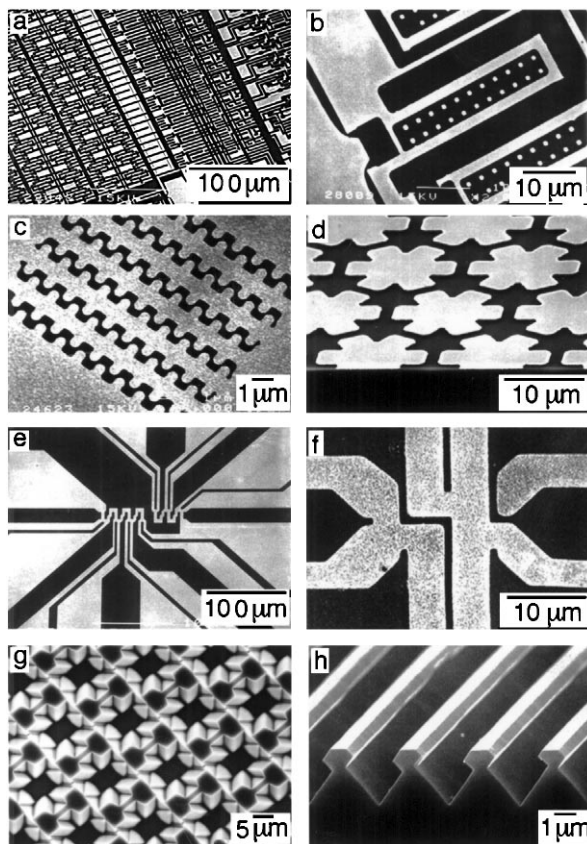


Figure 3 Scanning electron microscopy (SEM) images of test patterns of silver (*a–c*, 50 nm thick; *d*, 200 nm thick), gold (*e*, 20 nm thick), and copper (*f*, 50 nm thick) that were fabricated using μ CP with HDT, followed by wet chemical etching. The patterns in (*a*) and (*b*) were printed with rolling stamps (128); the patterns in (*c–f*) were printed with planar stamps (113, 116, 126). The bright regions are metals; the dark regions are Si/SiO₂ exposed where the etchant has removed the unprotected metals. (*g,h*) SEM images of silicon structures fabricated by anisotropic etching of Si(100), with patterned structures of silver or gold as resists (44, 133). The structure in (*h*) was generated using a combination of shadow evaporation and anisotropic etching of Si(100).

properties of SAMs, we and other groups have been able to pattern a wide variety of materials [for example, liquid prepolymers (134–136), conducting polymers (137–140), inorganic salts (141), metals (121, 142, 143), ceramics (144), and proteins (85, 145, 146)] using patterned SAMs as the templates to control the deposition. These processes use self-assembly at two scales: the formation of patterned SAMs at the molecular scale and the deposition of other materials on the patterned SAMs at the mesoscopic scale. Recently, Abbott

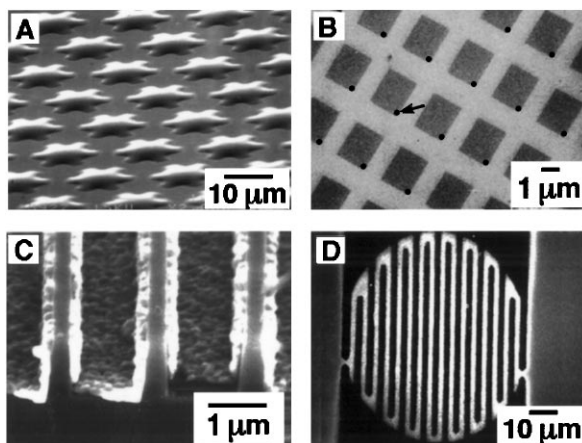


Figure 4 Selective wetting, nucleation, and deposition with patterned SAMs as templates: (a) An SEM image of microstructures of polyurethane (PU) assembled using selective dewetting (35). (b) An SEM image of microdots of CuSO_4 (arrow) formed by selective dewetting and crystallization (141). The dark squares are SAMs terminated in $-\text{COOH}$ groups; the light grids are SAMs terminated in $-\text{CH}_3$ groups. (c) An SEM image of microstructures of Cu (light) formed in Si microtrenches using selective CVD (142). (d) An SEM image of microstructures of LiNbO_3 (light) on Si/SiO_2 (dark) produced using selective CVD (144).

et al also used patterned SAMs formed by μCP to control both azimuthal and polar orientations of nematic liquid crystals (LCs) (147).

Figure 4a shows an SEM image of isolated stars of polyurethane (PU) fabricated using a combination of μCP and selective dewetting (35, 134). The liquid prepolymer of PU, when placed on a surface patterned with SAMs, selectively dewetted the hydrophobic (CH_3 -terminated) regions and formed patterned microstructures on the hydrophilic (COOH -terminated) regions (35). The liquid prepolymer selectively trapped in the hydrophilic regions was then cured under UV light. Figure 4b shows an SEM image of arrays of submicrometer-sized dots of CuSO_4 that were formed by selectively wetting a SAM-patterned surface of Au with an aqueous solution containing CuSO_4 , followed by evaporation of water (141). Using this simple approach, D Qin et al (unpublished data) have been able to form regular arrays of dots of CuSO_4 with lateral dimensions as small as ~ 50 nm.

Nuzzo et al have used patterned SAMs as templates to control the nucleation and growth of metals and ceramics by selective chemical vapor deposition (CVD) (121, 142–144). Figure 4c,d shows two examples: selective CVD of Cu and LiNbO_3 . The patterned SAMs defined and directed CVD by inhibiting nucleation, using CH_3 -terminated SAMs of alkylsiloxanes. The materials to be deposited only nucleated and grew on the bare regions (SiO_2) that were

not derivatized with hydrophobic (CH_3 -terminated) SAMs; nucleation on the polar regions formed patterned microstructures. These demonstrations suggest that μCP of SAMs, in combination with other processes, can be used to form patterned microstructures of a wide variety of materials.

MICROMOLDING AND RELATED TECHNIQUES

Replica Molding (REM)

Replica molding is an efficient method for the duplication of the information (i.e. shape, morphology, and structure) present in the surface of a mold (27). UV- or thermally curable prepolymers, as long as they do not contain solvent, usually have a shrinkage of less than 3% on curing; the cured polymers, therefore, possess almost the same dimensions and topologies as the channels in the PDMS mold. The fidelity of this process is largely determined by van der Waals interactions, wetting, and kinetic factors such as filling of the mold. These physical interactions are short range and should allow more accurate replication of small (<100 nm) features than does photolithography (148). The value of replica molding is as a replication method: It allows duplication of three-dimensional topologies in a single step; it also enables faithful duplication of complex structures in the master in multiple copies with nanometer resolution in a simple, reliable, and inexpensive way. Replica molding against a rigid mold with an appropriate material (usually a thermoplastic polymer) has been used for the mass-production of a wide range of structured surfaces such as compact disks (CDs) (27, 28), diffraction gratings (149), holograms (150), and micro-tools (151). We have extended the capability of this procedure by molding against elastomeric PDMS molds rather than against rigid molds; the use of elastomers makes it easier to release small, fragile structures.

Figure 5a outlines the procedure schematically (22, 152). The PDMS molds are prepared by casting against rigid masters using a procedure similar to that used in μCP . The relief features on the PDMS mold can, in turn, be faithfully replicated by using this structure as a mold for forming structures in a second UV-curable (or thermally curable) prepolymer. The relief structures on the replica are complementary to those on the mold and very similar to those on the original master. We have demonstrated replica molding against elastomeric PDMS molds with resolution <10 nm (153). Figure 6a, for example, shows the AFM image of Cr nanostructures on a master, and Figure 6b shows the AFM image of nanostructures in polyurethane (PU) prepared by replication against a PDMS mold cast from this master. The heights (peak to valley) of the Cr lines on the original master were ~ 13 nm; the heights of the PU lines were ~ 8 nm. These results indicated that replica molding against a PDMS mold is capable

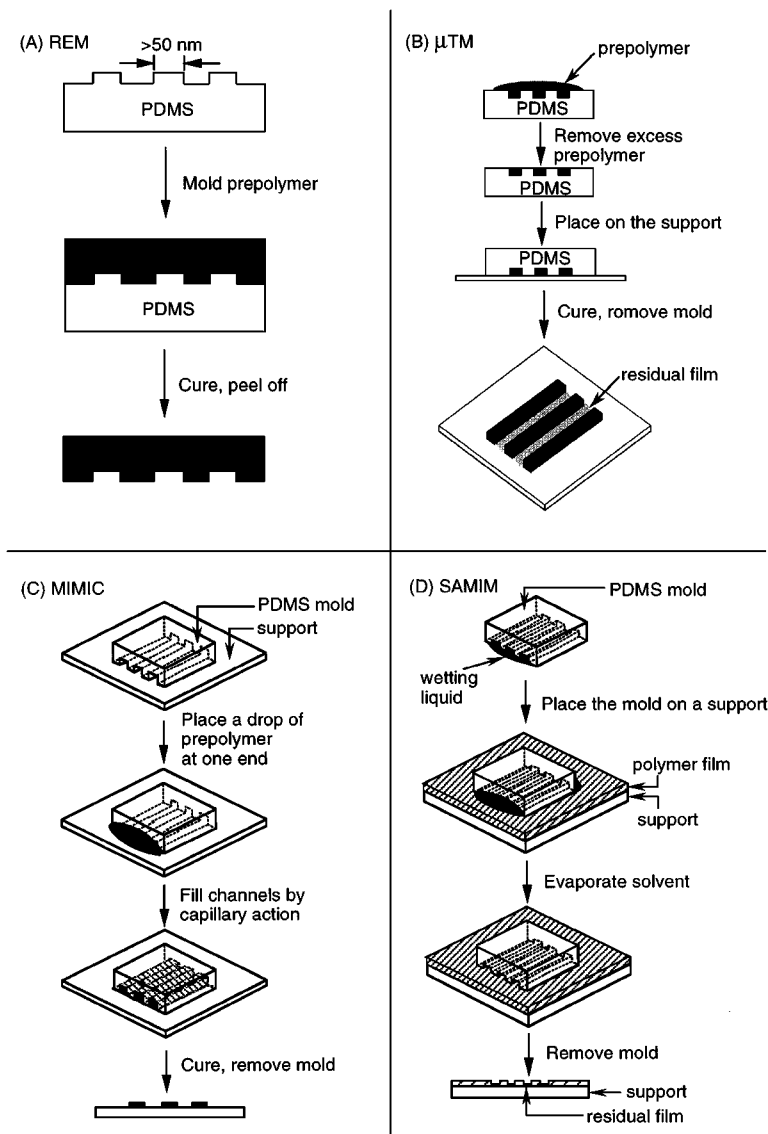


Figure 5 Schematic illustration of procedures for (a) replica molding (REM), (b) microtransfer molding (μ TM), (c) micromolding in capillaries (MIMIC), and (d) solvent-assisted micromolding (SAMIM).

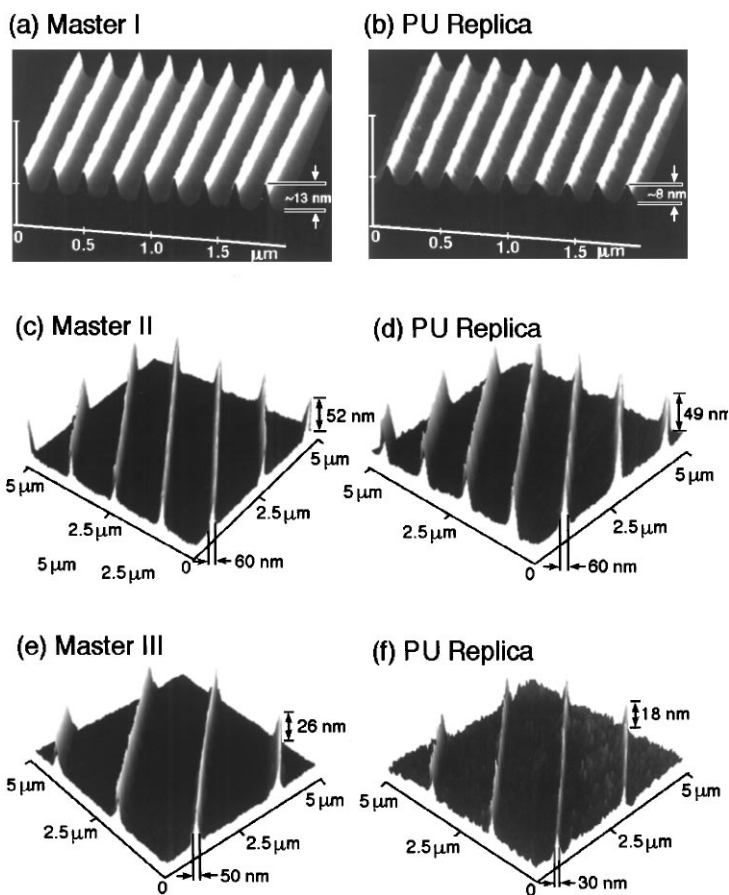


Figure 6 (a,b) Atomic force microscopy (AFM) images of Cr structures on a master, and a PU replica prepared from a PDMS mold cast from this master (153). (c,d) AFM images of Au structures on another master, and a PU replica produced from a PDMS mold cast from this master. (e,f) AFM images of Au structures on a third master, and a PU replica fabricated from a PDMS mold (cast from this master) while this mold was mechanically deformed by bending in a manner that generated narrower lines.

of reproducing the vertical dimension of nanostructures with an accuracy better than 5 nm over substantial areas ($\sim 1 \text{ mm}^2$) (153).

We also demonstrated that this procedure can be used to generate multiple copies of nanostructures starting from a single master (153). Figure 6c shows the AFM image of gold structures on another master before it was used to cast PDMS molds; Figure 6d shows the AFM image of nanostructures in PU fabricated by molding against a PDMS mold cast from this master. We

have monitored the quality of the structures of PU successively replicated from PDMS molds prepared from the same master. Because the procedures used for the preparation of both PDMS molds and PU replicas use an elastomer as one of the two materials, both master and mold can be repeatedly used a number of times (≥ 10) without observation of damage to the master or of degradation in the quality of the PU replicas. The simplicity and low cost of this procedure suggest its potential for use in manufacturing of nanometer-sized structures.

The sizes and shapes of features present in the surface of a PDMS mold can be manipulated in a controlled way by deforming this mold using mechanical compression, bending, stretching, or a combination of all (22). In this approach, the relief features in the surface of a PDMS mold are reconfigured by mechanical deformation and then replicated using cast molding. If desired, this procedure can be repeated, using the PU replica as the starting point, to make structures more complex than can be generated in one cycle (although with some degradation in the quality of the resulting structures). Figure 6e shows the AFM image of nanostructures of Au on a third master with a feature size of ~ 50 nm; Figure 6f shows the AFM image of a PU replica duplicated against a PDMS mold (cast from this master) while it was bent mechanically. The dimension of the features was reduced from ~ 50 to ~ 30 nm in this process (153).

Microtransfer Molding (μ TM)

In μ TM (Figure 5b), a thin layer of liquid prepolymer is applied to the patterned surface of a PDMS mold and the excess liquid is removed by scraping with a flat PDMS block or by blowing off with a stream of nitrogen (23). This mold, filled with the prepolymer, is then placed in contact with the surface of a substrate, and the prepolymer is cured to a solid by illuminating the mold with UV light or by heating it. When the mold is peeled away carefully, a patterned microstructure is left on the surface of the substrate. At its current state of development, microstructures fabricated by μ TM on a flat surface usually have a thin (~ 100 nm) film between the raised features. This thin film must be removed using O_2 RIE if the intent is to use the patterned microstructures as masks to control the etching of the underlying substrates.

Microtransfer molding can produce patterned microstructures of a wide variety of polymers (both pristine or doped with fluorescent dyes such as rhodamine 6G) over relatively large areas (~ 3 cm²) within a short period of time (~ 10 min). Zhao et al have used this technique to fabricate optical waveguides, couplers, and interferometers from organic polymers (23, 154). Figure 7a shows the top view of arrays of 3-cm long polymeric waveguides fabricated from UV-curable polyurethane using μ TM (23). Figure 7b shows a cross-sectional SEM image of these waveguides (23). These waveguides (with cross sections of ~ 3 μ m²) support multimode transmission of 633 and 488 nm

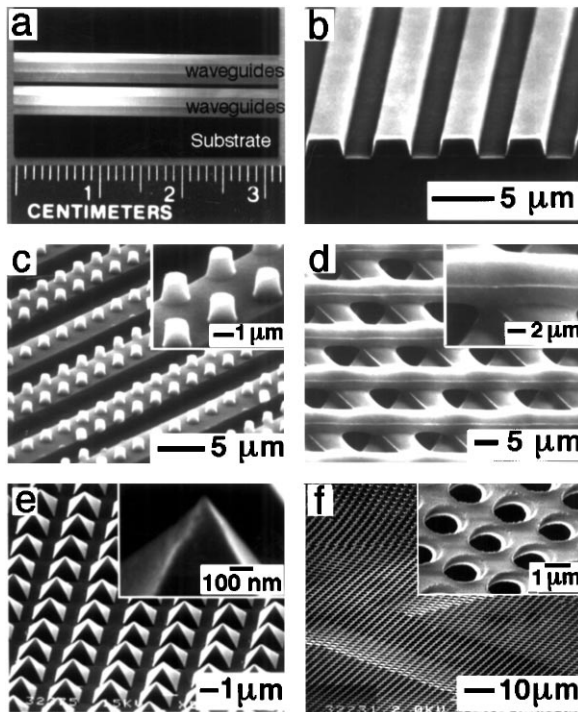


Figure 7 Polymeric microstructures fabricated using μ T M (23). (a) A photograph of arrays of 3-cm long waveguides of PU fabricated on Si/SiO₂. The waveguides have different lateral dimensions and are separated by different spacing. (b) An SEM image of the ends of the waveguides. (c) An SEM image of an array of isolated microcylinders of epoxy on 5- μ m lines of epoxy, supported on a glass slide. (d) An SEM image of a three-layer structure on a glass slide made from a thermally curable epoxy. (e,f) SEM images of microstructures of glasses fabricated by molding with sol-gel materials, followed by thermal consolidation.

light. Zhao et al have also fabricated arrays of optical couplers and interferometers by changing the separations between waveguides or by additional UV exposure after fabrication (154).

Microtransfer molding is capable of generating both interconnected and isolated microstructures. More importantly, μ T M can form microstructures on nonplanar surfaces; this characteristic enables the fabrication of three-dimensional microstructures layer by layer. Figure 7c,d shows two typical examples of three-dimensional structures that have been fabricated using μ T M (23). Figure 7c shows micro-posts of thermally curable epoxy fabricated on an array of parallel lines made of the same material. Figure 7d shows a three-layer

structure made of epoxy; the 4- μm wide lines are oriented at $\sim 60^\circ$ from each other. Microtransfer molding has also been used to form patterned microstructures of a variety of materials other than organic polymers: for example, glassy carbon, sol-gels, and ceramics (155–157). Figure 7e,f gives SEM images of microstructures (an array of square pyramids and a free-standing membrane, respectively) of glasses fabricated from sol-gel precursors (157).

Micromolding in Capillaries (MIMIC)

In MIMIC (Figure 5c), a PDMS mold is placed on the surface of a substrate to form a network of empty channels between them (24). A low-viscosity prepolymer is then placed at the open ends of the channels, and this liquid spontaneously fills the channels by capillary action. After curing the prepolymer into a solid, the PDMS mold is removed to reveal patterned microstructures of the polymer. Interestingly, capillaries with closed ends can also fill completely if they are short: The gas in them appears to escape by diffusing into the PDMS.

MIMIC is applicable to patterning a broader range of materials than is photolithography. We and other groups have successfully used a wide variety of materials in MIMIC, including UV-curable (or thermally curable) prepolymers that have no solvents (24, 158–160), and solutions or suspensions of structural or functional polymers (Y Xia, unpublished data), precursor polymers to glassy carbon (155, 156) or ceramics (Y Xia, unpublished data), sol-gel materials (158, 161, 162), inorganic salts (158), polymer beads (163), colloidal particles (158), and biologically functional macromolecules (164). When the solvents are removed by evaporation, the materials in the solutions or suspensions solidify within the confines of the channels and form patterned microstructures on the surface of the substrate. The resulting structures are usually thinner than the height of the channels in the PDMS mold but have approximately the same lateral dimensions.

Figure 8 illustrates the capability and feasibility of MIMIC. Figure 8a shows the SEM image of quasi-three-dimensional structures (structures with multiple thicknesses) of polyurethane fabricated by MIMIC (159). Such complex arrays of μm - and sub- μm -scale channels filled completely; in some regions of these structures, features are only connected to one another by channels with thicknesses < 100 nm. We note that MIMIC can form such patterned microstructures in a single step, whereas photolithography requires several steps of patterning. Figure 8b shows the SEM image of a line (in an array) of polyaniline formed by MIMIC from a solution of polyaniline emeraldine base in *N*-methyl-2-pyrrolidone (NMP) (Y Xia, unpublished data). This line was then converted into the conductive form of emeraldine salt by doping in an aqueous HCl solution. Figure 8c shows the SEM image of an array of lines of zirconia (ZrO_2) that was fabricated using MIMIC from the suspension of a

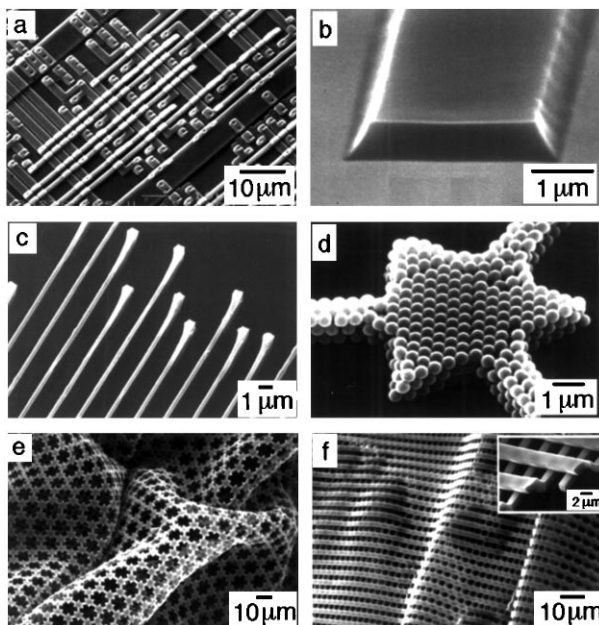


Figure 8 SEM images of microstructures of various materials fabricated using MIMIC (158, 159). (a) An SEM image of quasi-three-dimensional structures of PU formed on Si/SiO₂. (b–d) SEM images of patterned microstructures of polyaniline emeraldine HCl salt, zirconia (ZrO₂), and polystyrene beads, respectively, that were fabricated from their solutions or suspensions using MIMIC. (e,f) SEM images of free-standing microstructured membranes of polyurethane. The buckling occurred during sample preparation; the absence of fractures demonstrates their strength.

precursor polymer (ZO9303, Chemat Technology) in ethanol, and then converted into ZrO₂ by heating at ~600°C for ~10 h (Y Xia, unpublished data). The ends of the lines separated from the substrate during thermal conversion. Figure 8d shows the SEM image of polystyrene beads crystallized within the confinement of capillaries (163). The crystallization of the polystyrene beads occurred spontaneously when the solvent (water) was evaporated. We note that it would be extremely difficult to form patterned structures of these materials (e.g. polymer beads and ceramics) using photolithography. The ability to pattern these materials opens the door to a number of potential applications. The patterned microstructures of conducting polymers (Figure 8b), for example, may prove useful in the fabrication of flexible, all-plastic electronic and optoelectronic devices (165); and the closely packed assemblies of polymer beads (Figure 8d) are potentially useful in chromatography and diffractive optics (166).

We have also used MIMIC to fabricate free-standing microstructures of polymers. Figure 8e shows the SEM image of a free-standing microstructure of polyurethane (24). It was fabricated on a Si/SiO₂ substrate using MIMIC, followed by lift-off by dissolving the layer of SiO₂ in an aqueous HF/NH₄F solution. Figure 8f shows another approach to a free-standing structure (159); in this instance, the support used in MIMIC had relief patterns on its own surface. The two PDMS molds (each with a relief pattern of parallel lines on its own surface) were put together face to face, and the channels between these two PDMS molds were filled with a liquid prepolymer that was subsequently UV-cured into a solid. When the two PDMS molds were separated, the cross-linked polymeric microstructure remained on the surface of one of the molds and could then be easily released. This type of free-standing microstructure—comprising two interconnected layers, with an independent relief structure in each—can be fabricated using photolithography only with great difficulty.

MIMIC is a microfabrication method that can accommodate many materials. The smallest features we have generated using this procedure were parallel lines with cross-sectional dimensions of $\sim 0.1 \times 2 \mu\text{m}^2$ (a value set by the PDMS molds that were available for use with this work) and do not represent intrinsic limitations to the technique. MIMIC has several limitations at its current stage of development: (a) MIMIC requires a hydraulically connected network of capillaries, albeit one in which there are no isolated structures. (b) Capillary filling is rapid and complete over short distances (~ 1 cm). Over a large distance, however, the rate of filling decreases significantly owing to the viscous drag of the fluid in the capillary and the distance over which the fluid has to be transported. The forward ends of capillaries may fill incompletely if the hydraulic drag is sufficiently high (167). (c) The rate of filling also decreases as the cross-sectional dimension of the capillary decreases and as the interfacial free energy of the surface decreases (24). Although several groups have demonstrated that appropriate liquids could wet and fill nanometer-sized (< 50 nm in diameter) capillaries over a short distance (168, 169), the very slow filling of small capillaries may limit the usefulness of MIMIC in many types of nanofabrication unless new methods for liquid delivery are developed.

Solvent-Assisted Micromolding (SAMIM)

SAMIM (Figure 5d) generates relief structures in the surface of a material using a good solvent that can dissolve (or soften) the material without affecting the PDMS mold (25). We wet a PDMS mold with the solvent and bring it into contact with the surface of the substrate (typically an organic polymer). The solvent dissolves (or swells) a thin layer of the substrate, and the resulting fluid or gel is molded against the relief structures in the mold. When the solvent dissipates and evaporates, the fluid solidifies and forms a patterned

relief structure complementary to that in the surface of the mold. SAMIM shares an operational principle similar to that of embossing, but differs from this technique in that SAMIM uses a solvent instead of temperature to soften the material and uses an elastomeric PDMS mold rather than a rigid master to imprint patterns into the surface of the substrate.

SAMIM can be used with a wide variety of materials, although our initial demonstration has focused on organic polymers. The only requirement for SAMIM seems to be for a solvent that dissolves the substrate, and wets (but swells very little!) the surface of the PDMS mold. In general, the solvent should have a relatively high vapor pressure and a moderately high surface tension (e.g. methanol, ethanol, and acetone) to ensure rapid evaporation of the excess solvent and minimal swelling of the PDMS mold. Other materials can also be added into the solvent and subsequently be incorporated into the resulting microstructures. Solvents with low vapor pressures (e.g. ethylene glycol and dimethyl sulfoxide) are not well suited for SAMIM. Hydrophilic elastomers or surface modification of PDMS (for example, by plasma treatment) is required when solvents with high surface tensions (e.g. water) are used, because they only partially wet hydrophobic surfaces. SAMIM can replicate complex relief structures over large areas in a single step (Figure 9*a-c*).

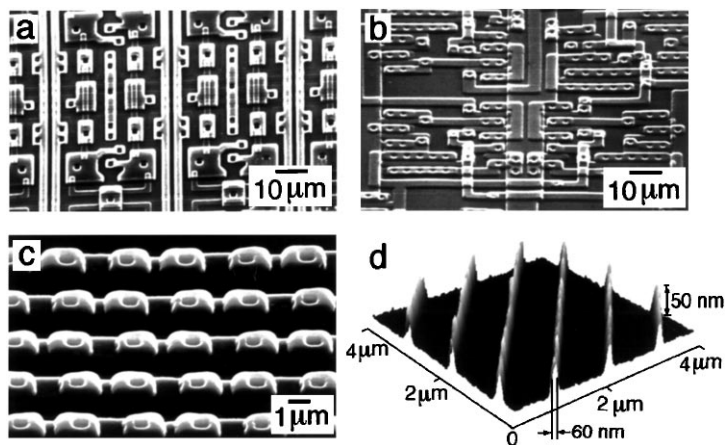


Figure 9 SEM and AFM images of polymeric microstructures fabricated using SAMIM (25). (*a-c*) SEM images of quasi-three-dimensional structures in photoresist (Microposit 1805, Shipley; $\sim 1.6 \mu\text{m}$ thick) spin-coated on Si/SiO_2 , polystyrene (PS, Goodfellow; $2.0 \mu\text{m}$ thick), and ABS (Goodfellow; $0.85 \mu\text{m}$ thick), respectively. (*d*) An AFM image of nanostructures in a thin ($\sim 0.4 \text{mm}$ thick) film of Microposit 1805 spin-coated on Si/SiO_2 . The solvent we used was ethanol for the photoresist and acetone for PS and ABS.

These quasi-three-dimensional structures are well defined and clearly resolved. Figure 9d shows an AFM image of the smallest features we have generated using SAMIM: Parallel lines ~ 60 nm wide and ~ 50 nm high formed in a thin film of Shipley photoresist (Microposit 1805, the thickness of the film was ~ 0.4 μm). A common characteristic of microstructures generated using SAMIM is that the resulting structures are joined by a thin, underlying film of the polymer. This film can be removed by homogeneous thinning using O_2 RIE, and the resulting polymeric structures can be used as masks in the etching of underlying substrates.

Embossing and Injection Molding

Embossing (27–29) and injection molding (170) form microstructures in thermoplastic polymers by imprinting the master into the thermally softened polymer or by injecting the softened polymer into the mold. Both techniques are cost-effective and high-throughput processes, and both are well-suited for manufacturing. The manufacturing of compact disks (CDs) based on imprinting in polycarbonate with a Ni master is a typical example of a large-volume commercial application of embossing (171). Recently, these two techniques have been explored seriously as methods for the production of nanometer-sized (< 50 nm) structures of semiconductors, metals, and other materials commonly used in microelectronic circuitry (30). Embossing, for example, has been used by Chou et al to generate features in Si with lateral dimensions as small as ~ 25 nm (172). This technique was also examined as a potential method for replicating binary optical components with features sizes < 100 nm (9, 28). The initial success of these two techniques and of soft lithographic techniques suggests that it will be useful to reexamine the potential of every existing microfabrication and high-resolution printing method for its potential in applications in high-resolution patterning.

APPLICATIONS OF SOFT LITHOGRAPHY

Soft lithography may offer immediate advantages in applications in which photolithography falters or fails. We and other groups have used soft lithographic techniques to fabricate a variety of functional components and devices in areas ranging from optics, through microanalysis, display, and MEMS, to microelectronics. We note that some of these devices cannot (or not easily) be fabricated using currently existing techniques based on photolithography. Here we show only three applications to highlight the potential of soft lithography: (a) formation of patterned microstructures on nonplanar surfaces, (b) fabrication of complex optically functional surfaces, and (c) fabrication of functional microelectronic devices.

Formation of Patterned Microstructures on Nonplanar Surfaces

Photolithography cannot be used to pattern even gently curved surfaces because of limitations to depth of focus (173). Microcontact printing with an elastomeric stamp provides an immediate route to patterning nonplanar surfaces, because it involves only conformal contact between the stamp and the surface of the substrate. Figure 2c illustrates an approach that Jackman et al have used to form patterned microfeatures on the surfaces of capillaries (174). Figure 10a shows the SEM image of a test pattern of Au that was fabricated by this procedure: μ CP with hexadecanethiol on gold-coated glass capillaries, followed by selective etching in an aqueous cyanide solution (174), with well-resolved submicron features of Au on a capillary having a diameter of $\sim 500 \mu\text{m}$. Jackman et al have also demonstrated that μ CP of alkanethiols on Au or Ag can generate micropatterns on both planar and nonplanar substrates with virtually the same edge resolution (174). Similar techniques have generated $3\text{-}\mu\text{m}$ lines of Au on $150\text{-}\mu\text{m}$ optical fibers (175). Xia et al recently also demonstrated that it is possible to form patterned microstructures on the inside surfaces of glass capillaries by using electroless deposition rather than metal evaporation to prepare the substrates (in this case, thin coatings of silver on the inside surfaces of capillaries), and an appropriately configured rolling stamp (115). These demonstrations open the door immediately to a wide range of new types of microstructures with potential applications in optical communication, MEMS, and microanalysis.

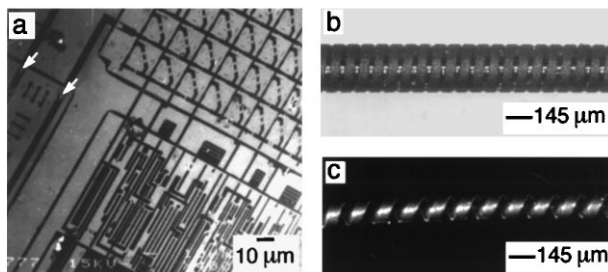


Figure 10 (a) The SEM image of test patterns of Au on the surface of a capillary that were fabricated using μ CP with HDT, followed by selective etching in an aqueous KCN solution saturated with O_2 (174). The arrows indicate two defects caused by sagging. (b,c) Optical micrographs of a microtransformer and a micro-spring fabricated by μ CP with HDT on silver (coated on the capillaries), followed by selective etching of silver and electroplating of (c) nickel and (d) copper (176, 178).

Rogers et al have further developed this procedure by introducing a monitoring and registration system into the experimental procedure. Using this modified procedure, they have successfully fabricated a wide range of functional structures and devices including in-fiber notch filters and Bragg gratings (175), microtransformers (see Figure 10*b*) (176), microcoils for high-resolution NMR spectroscopy (177), micro-springs (Figure 10*c*) (178), and intravascular stents (179).

Fabrication of Complex Optically Functional Surfaces

We can fabricate complex optically functional surfaces by replica molding against elastomeric molds while they are deformed mechanically (22). The highly isotropic deformation of the PDMS mold even allows patterned microstructures to be formed with gradients in size and shape. The capability and feasibility of this procedure has also been demonstrated by the production of (a) diffraction gratings with periods smaller than the original grating used as the master to cast the PDMS mold; (b) chirped, blazed diffraction gratings on planar and curved surfaces; (c) patterned microfeatures on the surfaces of approximately hemispherical objects; and (d) arrays of rhombic microlenses.

Xia et al fabricated chirped diffraction gratings (180)—gratings whose periods change continuously with position—by compressing one end of the elastomeric mold more than the other (22). The shape of the diffracting elements was largely preserved in this process: If we used a blazed grating as the starting master, the resulting chirped replica was also a blazed grating (Figure 11*a*). The period (Λ) of this chirped, blazed grating changed continuously from a value of ~ 1.55 to ~ 1.41 μm over a distance of ~ 0.9 cm; the rate of chirping ($d\Lambda/dz$) was $\sim 1.6 \times 10^{-5}$. This grating was characterized in transmission at normal incidence. Figure 11*b* shows the diffraction patterns (the zeroth-order and the two first-order peaks) of the PDMS mold, its replica, and the chirped replica. The first diffraction peak shifted continuously in position as the laser spot was scanned across the chirped grating along the Z direction.

Fabrication of Functional Microelectronic Devices

The use of soft lithographic methods to fabricate microelectronic devices represents one of the most stringent tests of their capabilities because this kind of fabrication requires multistep patterning and registration. We and other groups have just begun to explore these ideas. Nuzzo et al have fabricated ferroelectric capacitors of Pt/Pb(Zr,Ti)O₃/Pt using a combination of μCP and selective CVD (181). Hu et al have used MIMIC successfully to fabricate simple, electrically functional devices such as Schottky diodes (J Hu, unpublished data), GaAs/AlGaAs heterostructure field effect transistors (FETs) (182), and

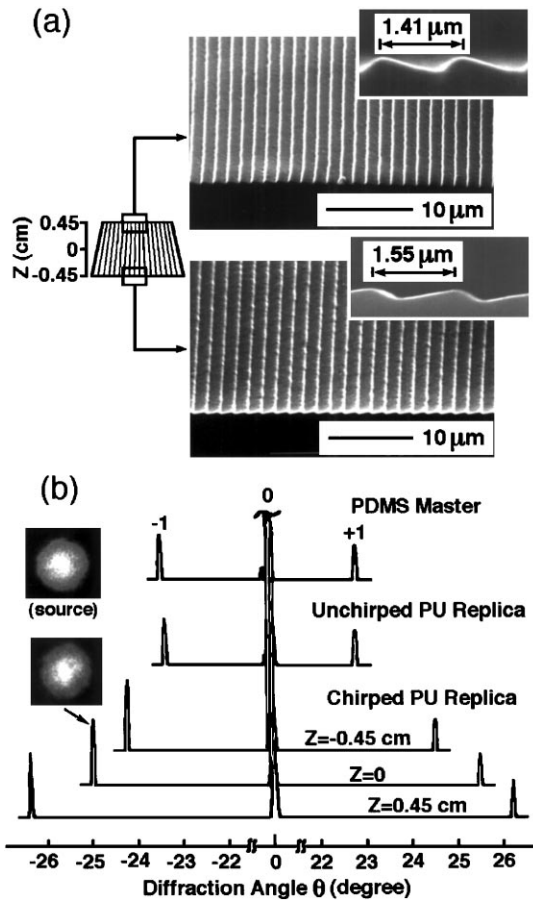


Figure 11 (a,b) Cross-sectional SEM images of selective regions of a planar, chirped, and blazed PU replica grating that was fabricated by molding against a PDMS mold while it was compressed asymmetrically (22). The PDMS mold was prepared by casting against a commercial blazed diffraction grating. (c) Diffraction patterns from the PDMS mold, its PU replica, and the chirped PU grating. A He-Ne laser ($\lambda = 632.8$ nm) was used.

Si MOSFETs (NL Jeon, unpublished data). The fabrication process for both types of transistors involved at least three steps of MIMIC, with registration between them. In each step, the pattern was defined by microstructures of PU formed using MIMIC: Etching and evaporation were performed using these patterned structures of PU as the masks. Figure 12a shows the oblique view of a GaAs/AlGaAs FET. The source and drain are AuNiGe ohmic contacts, the channel is defined by a mesa etch, and the gate is a Cr/Au Schottky contact.

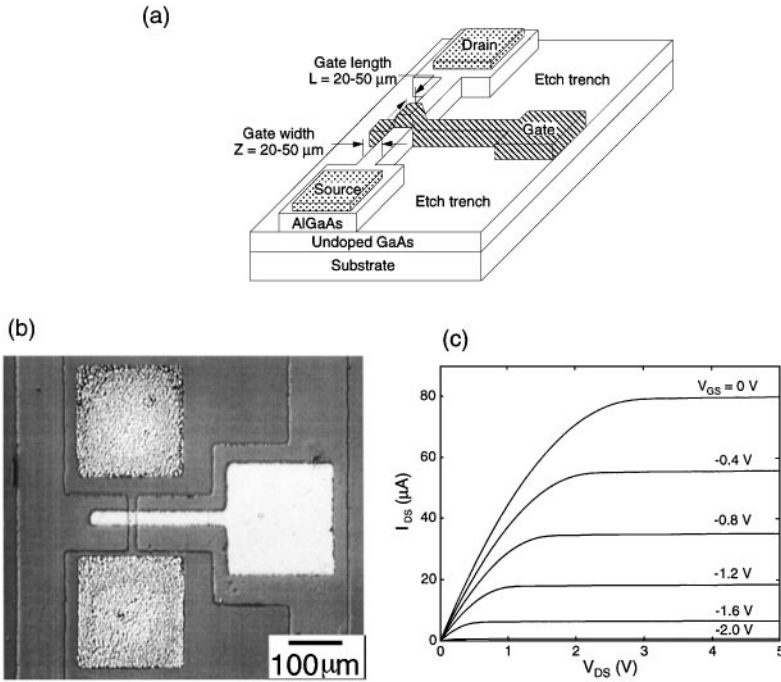


Figure 12 (a) Schematic diagram of a GaAs/AlGaAs FET. (b) Optical micrograph of a GaAs/AlGaAs FET ($L = 26 \mu\text{m}$ and $Z = 16 \mu\text{m}$) fabricated using MIMIC (182). (c) The performance of a representative GaAs/AlGaAs FET fabricated using this procedure.

Figure 12b shows an optical micrograph of the FET with $L = 26 \mu\text{m}$ and $Z = 16 \mu\text{m}$. Figure 12c shows the performance of a representative FET fabricated using this procedure. Its characteristics are similar to those of FETs fabricated using conventional photolithographic techniques. Although the feature sizes ($16\text{--}26 \mu\text{m}$) that characterize these devices are a factor of ~ 100 larger than those of state-of-the-art commercial devices ($\sim 250 \text{ nm}$), these results indicated that soft lithography can be used for multilayer fabrication that has, up to this time, been monopolized by photolithography; they also set a benchmark against which to measure further development in this area.

CONCLUSIONS

Microfabrication will certainly grow in importance in a wide range of areas: from microelectronics, through display, MEMS, sensing, optics, microanalysis, and combinatorial synthesis, to cell biology. Photolithography will, of course,

continue as the dominant technology in microfabrication of microelectronic systems for the foreseeable future. It is, however, not necessarily the best option for all tasks in patterning. The soft lithographic techniques explored by us, and the non-photolithographic techniques developed in other groups, offer immediate advantages in a number of applications: for example, patterning on scales <100 nm, patterning on nonplanar surfaces, patterning of solid materials other than photoresists, patterning of liquid materials, patterning of surface functionalities, patterning over large areas, and formation of three-dimensional microstructures and systems. Soft lithography may also become competitive with photolithography in conventional patterning processes in which the capital cost of equipment is the primary concern, or in which requirements for precise alignment, isolation, continuity, and uniformity in the final patterns are relaxed: for example, arrays of microelectrodes, diffractive optical components, simple display devices, MEMS, microanalytical systems, sensors, biosensors, and microreactors. Our recent successes in multilayer fabrication (albeit with accuracy in registration of only ~ 20 μm) (182) also suggest that rapid prototyping (183) of elementary devices for use in consumer electronics is now practical.

Soft lithography is still in an early stage of technical development. There are a number of issues that remain to be solved before soft lithography can compete with photolithography in the core application of microfabrication: that is, manufacturing of microelectronic circuitry. First, the deformation and distortion of the elastomeric stamp/mold during soft lithography must be completely understood and fully managed. Second, the properties of the elastomer must be optimized to make pattern transfer exactly reproducible, especially for features with very small sizes. Third, high-resolution registration (<20 nm) has to be demonstrated with the current or optimized elastomer. Fourth, the density of defects in the final patterns, especially in those formed by a combination of μCP and wet etching (184), must be well-characterized and kept below the level tolerated in microelectronics fabrication. Fifth, the compatibility of soft lithographic techniques with the processes used in the production of microelectronics chips still needs to be defined and improved. For microcontact printing, especially, new systems that can form SAMs directly on inorganic semiconductors rapidly and reproducibly have to be developed.

In broad terms, however, soft lithography and its derivative technologies represent a new (or more properly, freshly reexamined) approach to micropatterning. The techniques of soft lithography clearly complement those of photolithography and extend micropatterning into dimensions, materials, and geometries to which photolithography cannot, in practice, be applied. Some day, with development, soft lithography may even compete with photolithography in its core applications!

ACKNOWLEDGMENTS

This work was supported in part by the Office of Naval Research (ONR), the Defense Advanced Research Projects Agency (DARPA), the NSF (PHY-9312572), and the AROD (340-6468-1/DAAH04-95-1-0102). This work made use of MRSEC Shared Facilities supported by the NSF under award number DMR-9400396. We would like to thank our colleagues and collaborators for their many and essential contributions to this work.

Visit the Annual Reviews home page at
<http://www.AnnualReviews.org>.

Literature Cited

1. Barrett CR. 1993. *Mater. Res. Soc. Bull.* XVIII, No.7:3–10
2. Bryzek J. 1996. *SENSORS* July:4–38
3. Clark RA, Hieptas PB, Ewing AG. 1997. *Anal. Chem.* 69:259–63
4. Briceno G, Chang HY, Sun XD, Schultz PG, Xiang XD. 1995. *Science* 270:273–76
5. Bryzek J, Peterson K, McCulley W. 1994. *IEEE Spectrum* May:20–31
6. Manz A. 1996. *CHIMIA* 59:140–45
7. Kovacs GTA, Petersen K, Albin M. 1996. *Anal. Chem.* 68:407A–12
8. Wu MC, Lin LY, Lee SS, King CR. 1996. *Laser Focus World* February:64–68
9. Herzog HP, ed. 1997. *Micro-Optics: Elements, Systems and Applications*. London: Taylor & Francis
10. Moreau WM. 1988. *Semiconductor Lithography: Principles and Materials*. New York: Plenum
11. Brambley D, Martin B, Prewett PD. 1994. *Adv. Mater. Opt. Electron.* 4:55–74
12. Rai-Choudhury P, ed. 1997. *Handbook of Microlithography, Micromachining, and Microfabrication*. Bellingham, WA: SPIE Opt. Engineer. Press. Vol. 1
13. Levenson MD. 1995. *Solid State Technol.* February:57–66
14. Geppert L. 1996. *IEEE Spectrum* April: 33–38
15. Pease RFW. 1992. *J. Vac. Sci. Technol. B* 10:278–85
16. Cerrina F, Marrian C. 1996. *Mater. Res. Soc. Bull.* XXI, No. 12:56–62
17. Miller RD, Wallraff GM. 1994. *Adv. Mater. Opt. Electron.* 4:95–127
18. Xia Y. 1996. *Soft lithography: micro- and nanofabrication based on microcontact printing and replica molding*. PhD thesis. Harvard Univ., Cambridge. 307 pp.
19. Zhao X-M, Xia Y, Whitesides GM. 1997. *J. Mater. Chem.* 7:1069–74
20. Xia Y, Whitesides GM. 1998. *Angew. Chem. Int. Ed. Engl.* In press
21. Kumar A, Whitesides GM. 1993. *Appl. Phys. Lett.* 63:2002–4
22. Xia Y, Kim E, Zhao X-M, Rogers JA, Prentiss M, Whitesides GM. 1996. *Science* 273:347–49
23. Zhao X-M, Xia Y, Whitesides GM. 1996. *Adv. Mater.* 8:837–40
24. Kim E, Xia Y, Whitesides GM. 1995. *Nature* 376:581–84
25. Kim E, Xia Y, Zhao X-M, Whitesides GM. 1997. *Adv. Mater.* 9:651–54
26. Rogers JA, Paul KE, Jackman RJ, Whitesides GM. 1997. *Appl. Phys. Lett.* 70:2658–60
27. Haverkorn von Rijsewijk HC, Legierse PEJ, Thomas GE. 1982. *Philips Tech. Rev* 40:287–97
28. Terris BD, Mamin HJ, Best ME, Logan JA, Rugar D. 1996. *Appl. Phys. Lett.* 69:4262–64
29. Lehmann HW, Widmer R, Ebnoether M, Wokaun A, Meier M, Miller SK. 1983. *J. Vac. Sci. Technol. B* 1:1207–10
30. Chou SY, Krauss PR, Renstrom PJ. 1995. *Appl. Phys. Lett.* 67:3114–16
31. Masuda H, Fukuda K. 1995. *Science* 268: 1446–68
32. Hoyer P. 1996. *Adv. Mater.* 8:857–59
33. Huber TE, Luo L. 1997. *Appl. Phys. Lett.* 70:2502–4
34. Clarson SJ, Semlyen JA, eds. 1993. *Siloxane Polymers*. Englewood Cliffs, NJ: Prentice Hall
35. Xia Y, Tien J, Qin D, Whitesides GM. 1996. *Langmuir* 12:4033–38
36. Wilbur JL, Kim E, Xia Y, Whitesides GM. 1995. *Adv. Mater.* 7:649–52

37. Xia Y, Whitesides GM. 1995. *Adv. Mater.* 7:471–73
38. Xia Y, Whitesides GM. 1997. *Langmuir* 13:2059–67
39. Wilbur JL, Jackman RJ, Whitesides GM, Cheung EL, Lee LK, Prentiss MG. 1996. *Chem. Mater.* 8:1380–85
40. Rogers JA, Jackman RJ, Schueller OJA, Whitesides GM. 1996. *Appl. Opt.* 35:6641–47
41. Rogers JA, Qin D, Schueller OJA, Whitesides GM. 1996. *Rev. Sci. Instrum.* 67:3310–19
42. Qin D, Xia Y, Whitesides GM. 1997. *Adv. Mater.* 9:407–9
43. Rogers JA, Paul KE, Jackman RJ, Whitesides GM. 1998. *J. Vac. Sci. Technol. B.* In press
44. Qin D, Xia Y, Black AJ, Whitesides GM. 1998. *J. Vac. Sci. Technol. B.* In press
45. Ferguson GS, Chaudhury MK, Biebuyck HA, Whitesides GM. 1993. *Macromolecules* 26:5870–75
46. Chaudhury MK. 1995. *Biosens. Bioelectron.* 10:785–88
47. Delamarche E, Schmid H, Biebuyck HA, Michel B. 1997. *Adv. Mater.* 9:741–46
48. Rogers JA, Paul KE, Whitesides GM. 1998. *J. Vac. Sci. Technol. B.* Submitted
49. Voet A. 1952. *Ink and Paper in the Printing Process.* New York: Interscience
50. Lehn J-M. 1990. *Angew. Chem. Int. Ed. Engl.* 29:1304–19
51. Whitesides GM, Mathias JP, Seto CT. 1991. *Science* 254:1312–19
52. Creighton TE. 1983. *Proteins: Structures and Molecular Properties.* New York: Freeman
53. Sanger W. 1986. *Principles of Nucleic Acid Structures.* New York: Springer-Verlag
54. Ringsdorf H, Schlarb B, Venzmer J. 1988. *Angew. Chem. Int. Ed. Engl.* 27:113–58
55. Lindsey JS. 1991. *New J. Chem.* 15:153–80
56. Simanek EE, Mathias JP, Seto CT, Chin D, Mammen M, et al. 1995. *Acc. Chem. Res.* 28:37–44
57. Dimitov AS, Nagayama K. 1996. *Langmuir* 12:1303–11
58. Bowden N, Terfort A, Carbeck J, Whitesides GM. 1997. *Science* 276:233–35
59. Terfort A, Bowden N, Whitesides GM. 1997. *Nature* 386:162–64
60. Ulman A. 1991. *Introduction to Thin Organic Films: From Langmuir-Blodgett to Self-Assembly.* Boston: Academic
61. Bain CD, Whitesides GM. 1989. *Angew. Chem. Int. Ed. Engl.* 28:506–12
62. Gardner TJ, Frisbie CD, Wrighton MS. 1995. *J. Am. Chem. Soc.* 117:6927–33
63. Whitesides GM, Laibinis PE. 1990. *Langmuir* 6:87–96
64. Dubois LH, Nuzzo RG. 1992. *Annu. Rev. Phys. Chem.* 43:437–63
65. Ulman A. 1995. *Mater. Res. Soc. Bull.* June:46–51
66. Bishop AR, Nuzzo RG. 1996. *Curr. Opin. Coll. Interface Sci.* 1:127–36
67. Delamarche E, Michel B, Biebuyck HA, Gerber C. 1996. *Adv. Mater.* 8:719–29
68. Fenter P, Eisenberger P, Li J, Camillone N III, Bernasek S, et al. 1991. *Langmuir* 7:2013–16
69. Allara DL, Parikh AN, Rondelez F. 1995. *Langmuir* 11:2357–60
70. Wirth MJ, Fairbank RWP, Fatunmbi HO. 1997. *Science* 275:44–47
71. Linford MR, Fenter P, Eisenberger PM, Chidsey CED. 1995. *J. Am. Chem. Soc.* 117:3145–55
72. Bansal A, Li X, Lauer mann I, Lewis NS, Yi SI, Weinberg WH. 1996. *J. Am. Chem. Soc.* 118:7225–26
73. Schlenoff JB, Li M, Ly H. 1995. *J. Am. Chem. Soc.* 117:12528–36
74. Sheen CW, Shi J-X, Martensson J, Parikh AN, Allara DL. 1992. *J. Am. Chem. Soc.* 114:1514–15
75. Gu Y, Lin Z, Butera RA, Smentkowski VS, Waldeck DH. 1995. *Langmuir* 11:1849–51
76. Chadwick JE, Myles DC, Garrell RL. 1993. *J. Am. Chem. Soc.* 115:10364–65
77. Uvdal K, Persson I, Liedberg B. 1995. *Langmuir* 11:1252–56
78. Lee TR, Laibinis PE, Folkers JP, Whitesides GM. 1991. *Pure Appl. Chem.* 63:821–28
79. Hickman JJ, Laibinis PE, Auerbach DI, Zou C, Gardner TJ, et al. 1992. *Langmuir* 8:357–59
80. Tao Y-T, Lee M-T, Chang S-C. 1993. *J. Am. Chem. Soc.* 115:9547–55
81. Folkers JP, Gorman CB, Laibinis PE, Buchholz S, Whitesides GM, Nuzzo RG. 1995. *Langmuir* 11:813–24
82. Cao G, Hong H-G, Mallouk TE. 1992. *Acc. Chem. Res.* 25:420–27
83. Wasserman SR, Biebuyck HA, Whitesides GM. 1989. *J. Mater. Res.* 4:886–91
84. Kumar A, Biebuyck H, Whitesides GM. 1994. *Langmuir* 10:1498–11
85. López GP, Biebuyck HA, Hörter R, Kumar A, Whitesides GM. 1993. *J. Am. Chem. Soc.* 115:10774–81
86. Mrksich M, Whitesides GM. 1995. *TIBTECH* 13:228–35
87. Mrksich M, Whitesides GM. 1996. *Annu. Rev. Biophys. Biomol. Struct.* 25:55–78
88. Tolles WM. 1996. *Nanotechnology* 7:59–105

89. Wink T, Vanzuilen SJ, Bult A, Vanbennekon WP. 1997. *Analyst* 122:R43–50
90. Wilbur JL, Kumar A, Kim E, Whitesides GM. 1994. *Adv. Mater.* 6:600–4
91. Kumar A, Abbott NL, Kim E, Biebuyck HA, Whitesides GM. 1995. *Acc. Chem. Res.* 28:219–26
92. Xia Y, Zhao X-M, Whitesides GM. 1996. *Microelectron. Eng.* 32:255–68
93. Biebuyck HA, Larsen NB, Delamarche E, Michel B. 1997. *IBM J. Res. Dev.* 41:159–70
94. Huang J, Hemminger JC. 1993. *J. Am. Chem. Soc.* 115:3342–43
95. Tarlov MJ, Burgess DRF, Gillen G. 1993. *J. Am. Chem. Soc.* 115:5305–6
96. Tam-Chang S-W, Biebuyck HA, Whitesides GM, Jeon N, Nuzzo RG. 1995. *Langmuir* 11:4371–82
97. Wollman EW, Frisbie CD, Wrighton MS. 1993. *Langmuir* 9:1517–20
98. Pease AC, Solas D, Sullivan EJ, Cronin MT, Holmes CP, Fodor SPA. 1994. *Proc. Natl. Acad. Sci. USA* 91:5022–26
99. Dressick WJ, Calvert JM. 1993. *Jpn. J. Appl. Phys.* 32:5829–39
100. Chan KC, Kim T, Schoer JK, Crooks RM. 1995. *J. Am. Chem. Soc.* 117:5875–76
101. Lercel M, Tiberio RC, Chapman PF, Craighead HG, Sheen CW, et al. 1993. *J. Vac. Sci. Technol. B* 11:2823–28
102. Söndag-Huethorst JAM, van Helleputte HRJ, Fokkink LG. 1994. *Appl. Phys. Lett.* 64:285–87
103. Lercel MJ, Craighead HG, Parikh AN, Seshadri K, Allara AL. 1996. *Appl. Phys. Lett.* 68:1504–6
104. Gillen G, Wight S, Bennett J, Tarlov MJ. 1994. *Appl. Phys. Lett.* 65:534–36
105. Berggren KK, Bard A, Wilbur JL, Gillaspay JD, Helg AG, et al. 1995. *Science* 269:1255–57
106. Berggren KK, Younkin R, Cheung E, Prentiss M, Black AJ, et al. 1997. *Adv. Mater.* 9:52–55
107. Johnson KS, Berggren KK, Black AJ, Chu AP, Dekker NH, et al. 1996. *Appl. Phys. Lett.* 69:2773–75
108. Abbott NL, Folkers JP, Whitesides GM. 1992. *Science* 257:1380–82
109. Delamarche E, Hoole ACF, Michel B, Wilkes S, Despont M, et al. 1997. *J. Phys. Chem. B.* 101:9263–69
110. Biebuyck HA, Whitesides GM. 1994. *Langmuir* 10:4581–87
111. Larsen NB, Biebuyck H, Delamarche E, Michel B. 1997. *J. Am. Chem. Soc.* 119:3017–26
112. Xia Y, Whitesides GM. 1995. *J. Am. Chem. Soc.* 117:3274–75
113. Xia Y, Kim E, Whitesides GM. 1996. *J. Electrochem. Soc.* 143:1070–79
114. Yang XM, Tryk AA, Hasimoto K, Fujishima A. 1996. *Appl. Phys. Lett.* 69:4020–22
115. Xia Y, Venkateswaren N, Qin D, Tien J, Whitesides GM. 1998. *Langmuir*. In press
116. Xia Y, Kim E, Mrksich M, Whitesides GM. 1996. *Chem. Mater.* 8:601–3
117. Moffat TP, Yang H. 1995. *J. Electrochem. Soc.* 142:L220–22
118. Xia Y, Mrksich M, Kim E, Whitesides GM. 1995. *J. Am. Chem. Soc.* 117:9576–77
119. St. John PM, Craighead HG. 1996. *Appl. Phys. Lett.* 68:1022–24
120. Wang D, Thomas SG, Wang KL, Xia Y, Whitesides GM. 1997. *Appl. Phys. Lett.* 70:1593–95
121. Jeon NL, Finnie K, Branshaw K, Nuzzo RG. 1997. *Langmuir* 13:3382–91
122. Hidber PC, Helbig W, Kim E, Whitesides GM. 1996. *Langmuir* 12:1375–80
123. Hidber PC, Neeley PF, Helbig W, Whitesides GM. 1996. *Langmuir* 12:5209–15
124. Marzolin C, Terfort A, Tien J, Whitesides GM. 1998. *Thin Solid Films*. Submitted
125. Tsai JCC. 1988. In *VSLI Technology*, ed. SM Sze, pp. 272–26. New York: McGraw-Hill
126. Xia Y, Zhao X-M, Kim E, Whitesides GM. 1995. *Chem. Mater.* 7:2332–37
127. Vossen JL, Kern W, eds. 1978. *Thin Film Processes*. New York: Academic
128. Xia Y, Qin D, Whitesides GM. 1996. *Adv. Mater.* 8:1015–17
129. Wilbur JL, Biebuyck HA, MacDonald JC, Whitesides GM. 1995. *Langmuir* 11:825–31
130. Kim E, Kumar A, Whitesides GM. 1995. *J. Electrochem. Soc.* 142:628–33
131. Kim E, Whitesides GM, Freiler MB, Levy M, Lin JL, Osgood RM. 1996. *Nanotechnology* 7:266–69
132. Whidden TK, Ferry DK, Kozicki MN, Kim E, Wilbur JL, Whitesides GM. 1996. *Nanotechnology* 7:447–51
133. Xia Y, Whitesides GM. 1996. *Adv. Mater.* 8:765–68
134. Biebuyck HA, Whitesides GM. 1994. *Langmuir* 10:2790–93
135. Gorman CB, Biebuyck HA, Whitesides GM. 1995. *Chem. Mater.* 7:252–54
136. Kim E, Whitesides GM, Lee LK, Smith SP, Prentiss M. 1996. *Adv. Mater.* 8:139–42
137. Gorman CB, Biebuyck HA, Whitesides GM. 1995. *Chem. Mater.* 7:526–29
138. Hammond P, Whitesides GM. 1995. *Macromolecules* 28:7569–71
139. Sayre CN, Collard DM. 1997. *J. Mater. Chem.* 7:909–12

140. Huang Z, Wang P-C, MacDiarmid AG, Xia Y, Whitesides GM. 1998. *Langmuir*. In press
141. Palacin S, Hidber PC, Bourgoign J-P, Miramond C, Fermon C, Whitesides GM. 1996. *Chem. Mater.* 8:1316–25
142. Jeon NL, Nuzzo RG, Xia Y, Mrksich M, Whitesides GM. 1995. *Langmuir* 11: 3204–26
143. Jeon NL, Clem PG, Payne AA, Nuzzo RG. 1996. *Langmuir* 12:5350–55
144. Jeon NL, Clem PG, Nuzzo RG, Payne DA. 1995. *J. Mater. Res.* 10:2996–99
145. Singhvi R, Kumar A, López GP, Stephanopoulos GP, Wang DIC, Whitesides GM, Ingber DE. 1994. *Science* 264:696–98
146. Mrksich M, Chen CS, Xia Y, Dike LE, Ingber DE, Whitesides GM. 1996. *Proc. Natl. Acad. Sci. USA* 93:10775–78
147. Gupta VK, Abbott NL. 1997. *Science* 276:1533–36
148. Wuff G. 1995. *Angew. Chem. Int. Ed. Engl.* 34:1812–32
149. Hutley MC. 1982. *Diffraction Gratings*. New York: Academic
150. Nakano M, Nishida N. 1979. *Appl. Opt.* 18:3073–74
151. Kiewit DA. 1973. *Rev. Sci. Instrum.* 44: 1741–42
152. Whitesides GM, Xia Y. 1997. *Photonics Spectra* January:90–91
153. Xia Y, McClelland JJ, Gupta R, Qin D, Zhao X-M, et al. 1997. *Adv. Mater.* 9:147–49
154. Zhao X-M, Smith SP, Waldman SJ, Whitesides GM, Prentiss M. 1997. *Appl. Phys. Lett.* 71:1017–19
155. Schueller OJA, Brittain ST, Whitesides GM. 1997. *Adv. Mater.* 9:477–80
156. Schueller OJA, Brittain ST, Marzolin C, Whitesides GM. 1997. *Chem. Mater.* 9: 1399–6
157. Marzolin C, Smith SP, Prentiss M, Whitesides GM. 1998. *Adv. Mater.* Submitted
158. Kim E, Xia Y, Whitesides GM. 1997. *J. Am. Chem. Soc.* 118:5722–31
159. Xia Y, Kim E, Whitesides GM. 1996. *Chem. Mater.* 8:1558–67
160. Zhao X-M, Stoddart A, Smith SP, Kim E, Xia Y, et al. 1996. *Adv. Mater.* 8:420–24
161. Trau M, Yao N, Kim E, Xia Y, Whitesides GM, Aksay IA. 1997. *Nature* 390:674–76
162. Lochhead MJ, Yager P. 1997. *Mater. Res. Soc. Symp. Proc.* 444:105–10
163. Kim E, Xia Y, Whitesides GM. 1996. *Adv. Mater.* 8:245–47
164. Delamarche E, Bernard A, Schmid H, Michel B, Biebuyck HA. 1997. *Science* 276:779–81
165. Bao Z, Feng Y, Dodabalapur A, Raju VR, Lovinger AJ. 1997. *Chem. Mater.* 9: 1299–301
166. Weisman JM, Sunkara HB, Tse AS, Asher SA. 1996. *Science* 274:959–60
167. Kim E, Whitesides GM. 1997. *J. Phys. Chem. B* 101:855–63
168. Dujardin E, Ebbesen TW, Hiura H, Tanigaki K. 1994. *Science* 266:1850–52
169. Martin CR. 1994. *Science* 266:1961–66
170. Legierse PEJ, Pasman JHT. 1989. *Polymers in Information Storage Technology*. New York: Plenum
171. Winslow JS. 1976. *IEEE Trans. Consum. Electron.* November:318–26
172. Chou SY, Krauss PR, Renstrom PJ. 1996. *Science* 272:85–87
173. Deninger WD, Garner CE. 1988. *J. Vac. Sci. Technol. B* 6:337–40
174. Jackman RJ, L. Wilbur J, Whitesides GM. 1995. *Science* 269:664–66
175. Rogers JA, Jackman RJ, Whitesides GM, Wagener JL, Vengsarkar AM. 1997. *Appl. Phys. Lett.* 70:7–9
176. Jackman RJ, Rogers JA, Whitesides GM. 1997. *IEEE Trans. Mag.* 33:2501–3
177. Rogers JA, Jackman RJ, Whitesides GM, Olson DL, Sweedler JV. 1997. *Appl. Phys. Lett.* 70:2464–66
178. Rogers JA, Jackman RJ, Whitesides GM. 1997. *J. Microelec. Sys.* 6:184–92
179. Rogers JA, Jackman RJ, Whitesides GM. 1997. *Adv. Mater.* 9:475–77
180. Suzuki A, Tada K. 1980. *Thin Solid Films* 72:419–26
181. Jeon NL, Clem PG, Jung DY, Lin WB, Girolami GS, et al. 1997. *Adv. Mater.* 9: 891–95
182. Hu J, Beck RG, Deng T, Westervelt RM, Maranowski KD, et al. 1997. *Appl. Phys. Lett.* 71:2020–22
183. Qin D, Xia Y, Whitesides GM. 1996. *Adv. Mater.* 8:917–19
184. Zhao X-M, Wilbur JL, Whitesides GM. 1996. *Langmuir* 12:3257–64



CONTENTS

Jahn-Teller Phenomena in Solids, <i>J. B. Goodenough</i>	1
Isotropic Negative Thermal Expansion, <i>Arthur W. Sleight</i>	29
Spin-Dependent Transport and Low-Field Magnetoresistance in Doped Manganites, <i>J. Z. Sun, A. Gupta</i>	45
High Dielectric Constant Thin Films for Dynamic Random Access Memories (DRAM), <i>J. F. Scott</i>	79
Imaging and Control of Domain Structures in Ferroelectric Thin Films via Scanning Force Microscopy, <i>Alexei Gruverman, Orlando Auciello, Hiroshi Tokumoto</i>	101
InGaN-Based Laser Diodes, <i>Shuji Nakamura</i>	125
Soft Lithography, <i>Yunan Xia, George M. Whitesides</i>	153
Transient Diffusion of Beryllium and Silicon in Gallium Arsenide, <i>Yaser M. Haddara, John C. Bravman</i>	185
Semiconductor Wafer Bonding, <i>U. Gösele, Q.-Y. Tong</i>	215
Cathodic Arc Deposition of Films, <i>Ian G. Brown</i>	243
The Material Bone: Structure--Mechanical Function Relations, <i>S. Weiner, H. D. Wagner</i>	271
Science and Technology of High-Temperature Superconducting Films, <i>D. P. Norton</i>	299
IN SITU STUDIES OF THE PROPERTIES OF MATERIALS UNDER HIGH-PRESSURE AND TEMPERATURE CONDITIONS USING MULTI-ANVIL APPARATUS AND SYNCHROTRON X-RAYS, <i>J. B. Parise, D. J. Weidner, J. Chen, R. C. Liebermann, G. Chen</i>	349
STUDIES OF MULTICOMPONENT OXIDE FILMS AND LAYERED HETEROSTRUCTURE GROWTH PROCESSES VIA IN SITU, TIME-OF-FLIGHT ION SCATTERING AND DIRECT RECOIL SPECTROSCOPY, <i>Orlando Auciello, Alan R. Krauss, Jaemo Im, J. Albert Schultz</i>	375
Perovskite Thin Films for High-Frequency Capacitor Applications, <i>D. Dimos, C. H. Mueller</i>	397
RECENT DEVELOPMENTS IN CONDUCTOR PROCESSING OF HIGH IRREVERSIBILITY FIELD SUPERCONDUCTORS, <i>J. L. MacManus-Driscoll</i>	421
Point Defect Chemistry of Metal Oxide Heterostructures, <i>Sanjeev Aggarwal, R. Ramesh</i>	463
Processing Technologies for Ferroelectric Thin Films and Heterostructures, <i>Orlando Auciello, Chris M. Foster, Rammamoorthy Ramesh</i>	501
The Role of Metastable States in Polymer Phase Transitions: Concepts, Principles, and Experimental Observations, <i>Stephen Z. D. Cheng, Andrew Keller</i>	533
Processing and Characterization of Piezoelectric Materials and Integration into Microelectromechanical Systems, <i>Dennis L. Polla, Lorraine F. Francis</i>	563
Recent Advances in the Development of Processable High-Temperature Polymers, <i>Michael A. Meador</i>	599
High-Pressure Synthesis, Characterization, and Tuning of Solid State Materials, <i>J. V. Badding</i>	631